Nanomed Res J 10(2):171-178, Spring 2025

RESEARCH ARTICLE

Nitrazepam Detection and Adsorptive Removal by BN Nanocluster ($B_{12}N_{12}$): DFT Simulations

Zahra Rostami[1,*], Sheida Ahmadi[1], Parvaneh Dalir Kheirollahi Nezhad[1], Huseyn A. Imanov[2], Sumit Kaushal[3]

[1] Department of Chemistry, Payame Noor University, Tehran, Iran

[2] Faculty of Natural Sciences and Agriculture, Department of Chemistry, Nakhchivan State University, Nakhchivan, Azerbaijan

[3] Centre for Research Impact and Outcome, Chitkara University Institute of Engineering and Technology, Chitkara University, Rajpura, Punjab, India

ARTICLE INFO

Article History:
Received 14 Mar 2025
Accepted 22 May 2025
Published 01 Jun 2025

Keywords:
Nitrazepam
Adsorption
Removal
BN Nanocluster
Density functional theory
Detection

ABSTRACT

This study investigated the potential of the boron nitride nanocluster ($B_{12}N_{12}$) as an effective adsorbent and sensor for the removal and detection of the widely used benzodiazepine drug nitrazepam (NZ) using density functional theory (DFT) calculations. The interaction between NZ and $B_{12}N_{12}$ was analyzed in various orientations, revealing that the nanocluster exhibits a stronger affinity for the nitro functional group of NZ. The calculated negative values of adsorption energy, Gibbs free energy changes, and enthalpy changes confirm that the interaction is experimentally feasible, exothermic, and occurs spontaneously. Further analysis assessed the effects of temperature and the presence of water as a solvent, showing that the adsorption process is more favorable at lower temperatures and remains viable in an aqueous environment. Additionally, the bandgap of $B_{12}N_{12}$, initially measured at 6.664 eV, was significantly reduced to 3.121 eV upon NZ adsorption, reflecting a notable percentage change in the bandgap (-53.167%) and a substantial improvement in electrical conductivity. These findings suggest that $B_{12}N_{12}$ is a highly suitable candidate for use as both an adsorbent and a sensor in applications involving the removal and detection of NZ.

How to cite this article
Rostami Z., Ahmadi Sh., Dalir Kheirollahi Nezhad P., Imanov H.A., Kaushal S. Nitrazepam Detection and Adsorptive Removal by BN Nanocluster ($B_{12}N_{12}$): DFT Simulations. Nanomed Res J, 2025; 10(2): 171-178. DOI: 10.22034/nmrj.2025.02.008

INTRODUCTION

Nitrazepam (NZ, Fig. 1.), a widely used benzodiazepine derivative, has garnered significant attention due to its therapeutic applications in managing insomnia and anxiety disorders [1]. Its pharmacological efficacy stems from its ability to modulate gamma-aminobutyric acid (GABA) receptors, inducing sedative and hypnotic effects [2]. However, the widespread use of nitrazepam has also raised concerns regarding its environmental presence and potential adverse effects on ecosystems and human health [3]. Residual nitrazepam, often detected in wastewater and surface water, poses challenges due to its persistence, bioaccumulation potential, and toxicity [4]. Consequently, the development of effective strategies for detecting and removing nitrazepam from aqueous environments has become a critical area of research in environmental science and materials chemistry [4]. Traditional methods for detecting and removing pharmaceuticals, including nitrazepam, from water sources often involve techniques such as liquid chromatography [5], advanced oxidation processes [6], or adsorption using activated carbon [2]. While these approaches have shown promise, they are often limited by high operational costs, complex procedures, and incomplete removal efficiency [7]. As a result, researchers have turned to nanotechnology as a viable alternative for addressing these challenges [8]. Nanomaterials, owing to their unique

* Corresponding Author Email: *rostami@pnu.ac.ir*

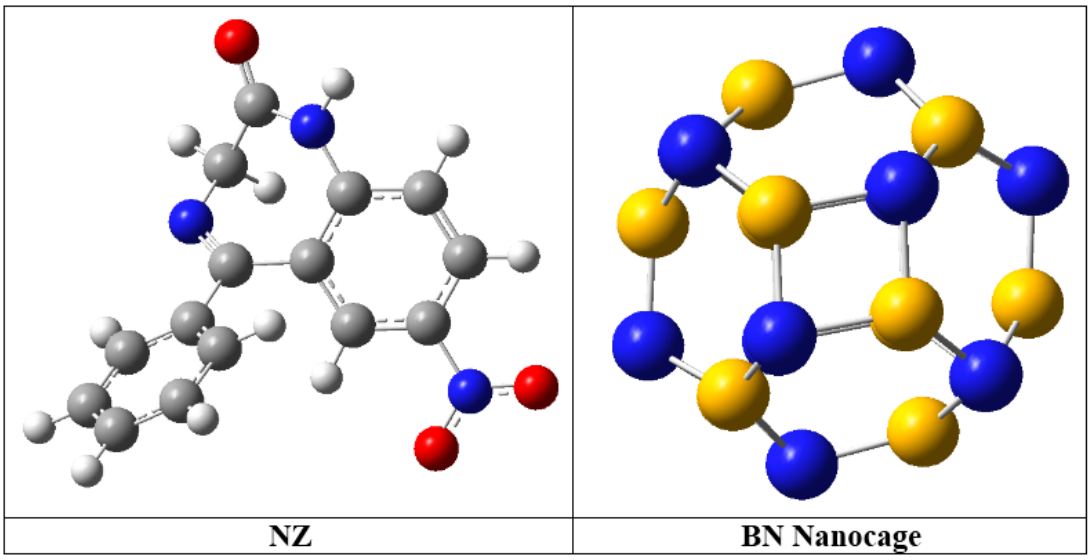

Fig. 1. Optimized structures of NZ and $B_{12}N_{12}$ (gray: carbon, white: hydrogen, blue: nitrogen, yellow: boron)

physicochemical properties, high surface area, and tunable reactivity, offer innovative solutions for both sensing and adsorptive removal of contaminants [9]. Among the diverse array of nanomaterials explored, boron nitride (BN) nanoclusters have emerged as a promising candidate due to their exceptional chemical stability, biocompatibility, and adsorption capabilities [10-12]. Boron nitride nanoclusters, specifically the $B_{12}N_{12}$ cluster (Fig.1.), have attracted considerable interest in recent years for their versatile applications in environmental remediation and molecular sensing [13]. Structurally composed of alternating boron and nitrogen atoms arranged in a cage-like geometry, the $B_{12}N_{12}$ nanocluster exhibits remarkable electronic properties that make it suitable for interacting with a wide range of organic molecules [14]. The polar nature of the boron-nitrogen bond imparts high affinity toward polar and aromatic compounds, making BN nanoclusters particularly effective for adsorbing pharmaceuticals such as nitrazepam [15]. Furthermore, density functional theory (DFT) simulations have emerged as a powerful computational tool for investigating the molecular interactions between BN nanoclusters and target analytes at an atomic level [16-18]. DFT simulations provide critical insights into adsorption mechanisms, binding energies, charge transfer processes, and electronic structure modifications, enabling researchers to design optimized nanomaterials for specific applications [19-22]. In this study, we aim to explore the potential of the $B_{12}N_{12}$ nanocluster as an advanced material for nitrazepam detection and adsorptive removal using DFT simulations [23]. By leveraging computational modeling techniques, we seek to elucidate the interaction dynamics between nitrazepam molecules and the BN nanocluster surface [24-26]. Specifically, we focus on understanding the adsorption behavior, electronic structure changes, and thermodynamic feasibility of the interaction [27-30]. The findings from this study are expected to contribute to the development of cost-effective and environmentally sustainable methods for mitigating pharmaceutical contamination in water systems. The significance of this research lies not only in addressing environmental pollution but also in advancing the broader field of nanotechnology-based remediation strategies. By demonstrating the applicability of $B_{12}N_{12}$ nanoclusters for nitrazepam detection and removal, this study underscores the potential of BN-based materials in tackling emerging contaminants. Moreover, the integration of DFT simulations into materials design highlights the importance of computational approaches in optimizing nanomaterials for real-world applications. As global concerns regarding water quality intensify, innovative solutions such as BN nanoclusters offer a promising pathway toward safeguarding environmental health while fostering interdisciplinary collaboration between chemistry, materials science, and environmental engineering.

Computational Methods

The structural design and evaluation of NZ, $B_{12}N_{12}$, and their combinations were meticulously carried out using GaussView 6 [31] and Nanotube Modeler 1.3.0.3. The procedure commenced with the geometric optimization of each structure to ensure stability and facilitate accurate subsequent analyses. Following optimization, a range of computational analyses was conducted, including infrared (IR) spectroscopy, and frontier molecular orbital (FMO) assessments. The Gaussian 16 software suite [32], known for its robust quantum chemical methodologies, was utilized for computational simulations. Additionally, density of states (DOS) spectra were determined using GaussSum 03. Density Functional Theory (DFT) [33] served as the primary computational approach to study the interaction between sertraline and the boron nitride nanocluster ($B_{12}N_{12}$). DFT, a quantum mechanical modeling method, calculates electronic structures by solving the Kohn-Sham equations and is particularly effective for examining adsorption processes due to its balance of computational efficiency and accuracy for systems with moderate to large molecular structures. For this study, the 6-31G* basis set [34] was selected for all calculations. This split-valence basis set incorporates polarization functions on heavy atoms, which are crucial for accurately describing electronic distributions and interaction energies in systems involving heteroatoms such as boron and nitrogen. The 6-31G* basis set offers an optimal balance between computational cost and precision, making it suitable for investigating adsorption phenomena on nanoclusters. The exchange-correlation functional employed in this study was the B3LYP [33] hybrid functional, which integrates Becke's three-parameter exchange functional with the Lee-Yang-Parr correlation functional. The B3LYP functional is widely recognized in computational chemistry for its reliable prediction of molecular properties, including adsorption energies and thermodynamic parameters. Calculations were performed in both gaseous and aqueous phases using the Conductor-like Polarizable Continuum Model (CPCM) to account for solvation effects [35]. Thermodynamic parameters were calculated at three different temperatures: 298 K, 308 K, and 318 K.

The process examined by [35] is as follows:

$$NZ + B_{12}N_{12} \rightarrow NZ\text{-}B_{12}N_{12} \quad (1)$$

RESULTS AND DISCUSSION

Structural Analysis

The interaction between NZ and $B_{12}N_{12}$ was analyzed from various orientations and conformers to identify the most stable configurations. Among the examined conformers, three were determined to be the most stable, as depicted in Fig. 2. In the A-Conformer, the adsorbent is positioned near the Nitro group of NZ. For the B-Conformer, the nanostructure aligns parallel to the benzodiazepine ring of NZ, while in the C-Conformer, $B_{12}N_{12}$ is situated close to the benzene ring of the adsorbate. Following geometrical optimization across all configurations, it was observed that the nanocluster moved closer to the NZ structure, suggesting a favorable interaction between NZ and $B_{12}N_{12}$. Additionally, no significant structural distortions were observed during optimization, indicating that the adsorption process is relatively weak and likely characterized as physisorption [36-38]. To further understand the adsorption behavior, the calculated adsorption energies are provided in Table 1. The adsorption energy values for all conformers are negative, confirming the experimental feasibility of NZ interacting with the BN nanocage. Upon closer examination of Table 1, it is evident that the A-Conformer is more favorable compared to B and C due to its more negative total electronic and adsorption energy values [39-43]. The influence of water as a solvent on adsorption energies was also investigated, revealing that while the adsorption energies become less negative in the presence of water, they remain negative overall. This indicates that NZ adsorption is still achievable in an aqueous environment, and water as a solvent does not significantly impact the interactions [44-46]. Additionally, the minimum and maximum calculated IR frequencies, as presented in Table 1, show no negative values, confirming that all analyzed structures correspond to true local minima. Another parameter evaluated was the dipole moment, which, as shown in Table 1, increases substantially after NZ interacts with the BN nanocage. This suggests that NZ-$B_{12}N_{12}$ complexes are more chemically reactive than the unmodified drug without the nanostructure [47-49].

Thermodynamic properties

To better understand the adsorption characteristics, thermodynamic parameters such as ΔH_{ad}, ΔG_{ad}, ΔS_{ad}, and K_{th} were determined for all conformers in both gaseous and aqueous environments at three different temperatures.

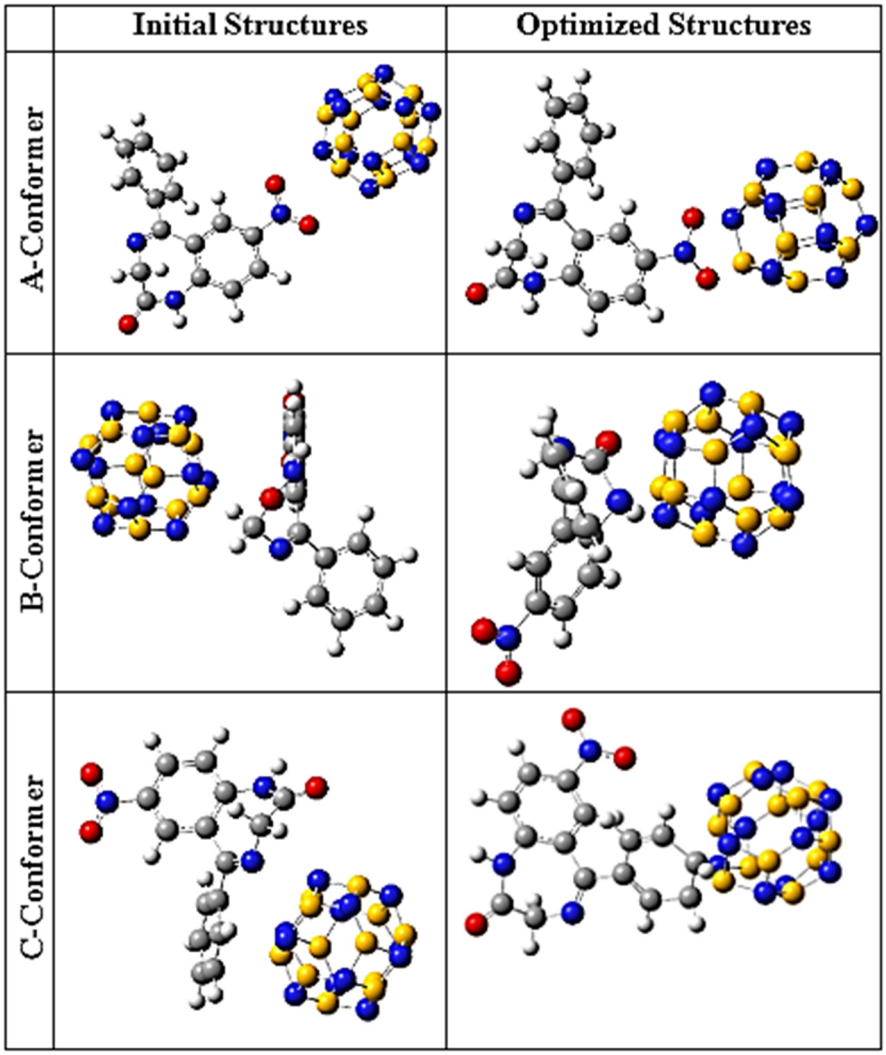

Fig. 2. Initial and optimized structures of NZ-$B_{12}N_{12}$ Complexes (gray: carbon, white: hydrogen, blue: nitrogen, yellow: boron)

Table 1. The structural properties of NZ, $B_{12}N_{12}$ and their complexes in gaseous and aqueous phases at room temperature

Structures	Total electronic energy (a.u)	Adsorption energy (kJ/mol)	ν_{min} (cm^{-1})	ν_{max} (cm^{-1})	Dipole moment (Deby)
NZ (Vacuum)	-968.095	---	96.951	4069.429	4.520
NZ (Water)	-968.103	---	92.243	4074.321	4.880
$B_{12}N_{12}$ (Vacuum)	-956.165	---	537.350	1795.870	0.000
$B_{12}N_{12}$ (Water)	-956.169	---	531.090	1792.220	0.030
A-Conformer (Vacuum)	-1924.282	-57.761	26.957	4001.693	5.640
A-Conformer (Water)	-1924.284	-31.506	29.171	4123.612	5.970
B-Conformer (Vacuum)	-1924.276	-42.008	34.412	4068.730	6.370
B-Conformer (Water)	-1924.279	-18.379	39.568	4089.159	6.630
C-Conformer (Vacuum)	-1924.268	-21.004	42.526	4091.677	7.120
C-Conformer (Water)	-1924.274	-5.251	41.545	4091.712	7.050

Table 2. The calculated thermodynamic parameters in both gaseous and aqueous phases in temperature range of 298-318 K at 10° intervals

Structures	ΔH_{ad} (kJ/mol)	ΔG_{ad} (kJ/mol)	ΔS_{ad} (J/mol)	K_{th}
A-Conformer-Vacuum-298	-53.435	-42.720	-63.379	$3.052\times10^{+07}$
A-Conformer-Vacuum-308	-51.635	-40.415	-65.939	$7.096\times10^{+06}$
A-Conformer-Vacuum-318	-49.835	-38.110	-68.499	$1.808\times10^{+06}$
A-Conformer-Water-298	-37.551	-16.835	-45.370	$8.903\times10^{+02}$
A-Conformer-Water-308	-35.751	-14.530	-47.580	$2.905\times10^{+02}$
A-Conformer-Water-318	-33.951	-12.225	-49.560	$1.017\times10^{+02}$
B-Conformer-Vacuum-298	-49.481	-48.410	-46.148	$3.031\times10^{+08}$
B-Conformer-Vacuum-308	-47.681	-46.105	-48.599	$6.540\times10^{+07}$
B-Conformer-Vacuum-318	-45.881	-43.800	-49.817	$1.554\times10^{+07}$
B-Conformer-Water-298	-15.847	-14.776	-58.321	$3.880\times10^{+02}$
B-Conformer-Water-308	-14.047	-12.471	-60.170	$1.300\times10^{+02}$
B-Conformer-Water-318	-12.247	-10.166	-60.743	$4.668\times10^{+01}$
C-Conformer-Vacuum-298	-49.481	-48.410	-46.148	$3.031\times10^{+08}$
C-Conformer-Vacuum-308	-47.681	-46.105	-48.599	$6.540\times10^{+07}$
C-Conformer-Vacuum-318	-45.881	-43.800	-49.817	$1.554\times10^{+07}$
C-Conformer-Water-298	-15.847	-14.776	-58.321	$3.880\times10^{+02}$
C-Conformer-Water-308	-14.047	-12.471	-60.170	$1.300\times10^{+02}$
C-Conformer-Water-318	-12.247	-10.166	-60.743	$4.668\times10^{+01}$

The findings are summarized in Table 2. The negative values of ΔH_{ad} and ΔG_{ad} indicate that the adsorption of NZ on the BN nanocage is exothermic and occurs spontaneously in both gaseous and aqueous phases. However, the negative ΔS_{ad} values suggest that the process is not entropy-favorable, implying that aggregation takes place within the NZ-$B_{12}N_{12}$ complexes following interaction [40]. Additionally, calculations of thermodynamic equilibrium constants revealed that the adsorption process is fully reversible and exists in an equilibrium state. The influence of temperature on these thermodynamic parameters was also examined, showing that as the temperature rises from 298 K to 318 K, ΔH_{ad} and ΔG_{ad} slightly increase, ΔS_{ad} becomes more negative, and K_{th} decreases significantly. Overall, these results suggest that the adsorption process is more thermodynamically favorable at lower temperatures [41].

FMO Analysis

The density of states (DOS) spectra for $B_{12}N_{12}$ and its complexes with NZ are illustrated in Fig. 3. The analysis reveals that the pristine BN nanocage possesses a bandgap of 6.664 eV. However, upon adsorption of NZ onto its surface, the bandgap decreases significantly to 4.093 eV, 3.121 eV, and 3.156 eV for A, B, and C conformers, respectively, corresponding to percentage changes in the bandgap (%ΔEg) of -38.573%, -53.167%, and -52.641%, respectively. This notable reduction in the bandgap of $B_{12}N_{12}$ after interaction with NZ suggests a substantial enhancement in its electrical conductivity, as conductivity is inversely proportional to the bandgap. Consequently, the BN nanocage demonstrates potential as a sensing material for the electrochemical detection of NZ [42].

Additionally, the chemical hardness of NZ, initially measured at 2.617 eV, decreases to 2.047 eV, 1.560 eV, and 1.578 eV for the A, B, and C conformers upon interaction with the BN nanocage, indicating improved chemical reactivity during the adsorption process. The negative values of chemical potential confirm that these structures are thermodynamically stable and favorable for such interactions. Furthermore, the indices for electrophilicity and maximum charge transfer capacity of NZ show a significant increase after adsorption on the $B_{12}N_{12}$ surface, highlighting an enhanced tendency of the molecule to accept electrons [43]. This implies that the NZ- $B_{12}N_{12}$ complexes exhibit greater electrophilic behavior compared to the unmodified NZ molecule, underscoring the potential utility of these complexes in applications requiring heightened electron absorption capabilities [44].

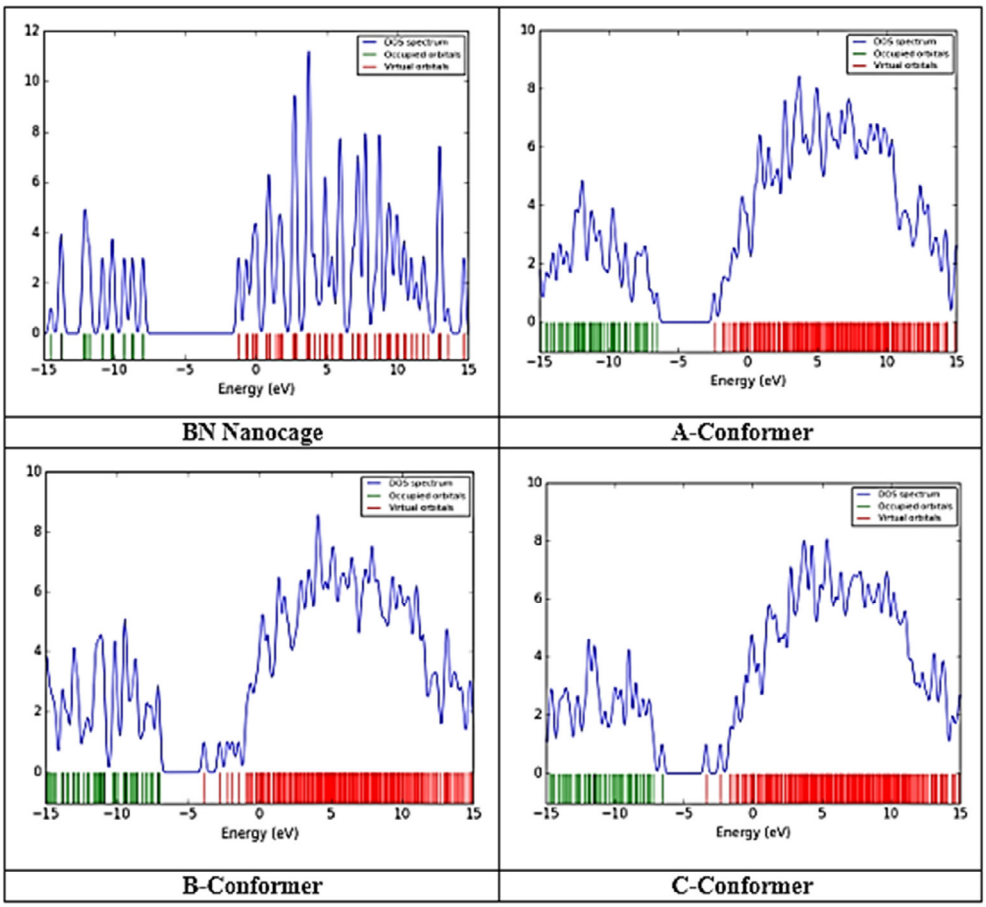

Fig. 3. DOS spectrums of $B_{12}N_{12}$ and its complexes with NZ

Table 3. The calculated FMO parameters

Structures	E_{HOMO} (eV)	E_{LUMO} (eV)	Eg (eV)	%ΔEg	η (eV)	μ (eV)	ω (eV)	ΔN_{max} (eV)
NZ	-7.553	-2.319	5.234	---	2.617	-4.936	4.655	1.886
$B_{12}N_{12}$	-7.893	-1.229	6.664	---	3.332	-4.561	3.122	1.369
A-Conformer	-6.491	-2.397	4.093	-38.573	2.047	-4.444	4.824	2.171
B-Conformer	-6.989	-3.868	3.121	-53.167	1.560	-5.428	9.442	3.479
C-Conformer	-6.532	-3.376	3.156	-52.641	1.578	-4.954	7.777	3.140

CONCLUSION

This research delves into the promising potential of the boron nitride nanocluster, specifically $B_{12}N_{12}$, as an efficient adsorbent and sensor for the removal and detection of the widely used benzodiazepine drug nitrazepam (NZ). By employing advanced density functional theory (DFT) calculations, the study meticulously analyzed the interaction between NZ molecule and the $B_{12}N_{12}$ nanocluster in various orientations. The findings revealed that $B_{12}N_{12}$ exhibits a particularly strong affinity for the Nitro group present in NZ, highlighting its selective adsorption capabilities. The calculated adsorption energy values, coupled with negative Gibbs free energy changes and enthalpy changes, unequivocally demonstrated that the interaction is not only experimentally feasible but also thermodynamically favorable, exothermic, and occurs spontaneously under standard conditions. Further investigations explored the influence of external factors such as temperature and the presence of water as a solvent. Results indicated that lower temperatures enhance

the adsorption process, while the interaction remains robust and viable even in an aqueous environment, underscoring its practical applicability in real-world scenarios. Additionally, a detailed analysis of the electronic properties of $B_{12}N_{12}$ revealed significant changes upon NZ adsorption. The pristine nanocluster's bandgap, initially measured at 6.664 eV, was significantly reduced to 3.121 eV after adsorption, marking a substantial percentage decrease of 53.167%. This reduction in bandgap corresponds to a notable improvement in the material's electrical conductivity, further enhancing its functionality as a sensor. Collectively, these findings strongly suggest that $B_{12}N_{12}$ is an excellent candidate for dual applications: as an adsorbent for removing NZ from environments and as a sensitive sensor for detecting its presence.

CONFLICT OF INTEREST

The authors declare that they have no conflicts of interest related to this work.

REFERENCES

1. Mahdi MI, Kadhim KH. A batch and cloud point extraction kinetic spectrophotometric method for determining trace and ultra trace amounts of Benzodiazepine drugs (Clonazepam and Nitrazepam) in pure and pharmaceutical preparations. Issues Pharm Med Sci. 2020;33:21-31. https://doi.org/10.2478/cipms-2020-0006
2. Nazal MK, Rao D, Abuzaid N. First investigations on removal of nitrazepam from water using biochar derived from macroalgae low-cost adsorbent: kinetics, isotherms and thermodynamics studies. Water Pract Technol. 2021;16:946-60.https://doi.org/10.2166/wpt.2021.040
3. Saito K, Yokota M, Ito R, Sakamoto M, Higashiyama K. Elucidation of degradation behavior of nitrazepam, a benzodiazepine drug, under basic conditions: study on degradability of drugs in stomach (IV). Chem Pharm Bull. 2024;72:11-5. https://doi.org/10.1248/cpb.c23-00626
4. Aboul-Enein HY, Jado AI, Loutfy MA. Nitrazepam. In: Florey K, editor. Analytical Profiles of Drug Substances. Vol 9. Academic Press; 1981. p. 487-517. https://doi.org/10.1016/S0099-5428(08)60151-3
5. Boukhabza A, Lugnier AA, Kintz P, Mangin P. Simultaneous HPLC analysis of the hypnotic benzodiazepines nitrazepam, estazolam, flunitrazepam, and triazolam in plasma. J Anal Toxicol. 1991;15:319-22. https://doi.org/10.1093/jat/15.6.319
6. Kosjek T, Perko S, Zupanc M, Hren MZ, Dragičević TL, Žigon D, et al. Environmental occurrence, fate and transformation of benzodiazepines in water treatment. Water Res. 2012;46:355-68. https://doi.org/10.1016/j.watres.2011.10.056
7. Coslop TF, Nippes RP, Bergamasco R, Scaliante MH. Evaluation of diazepam adsorption in aqueous media using low-cost and natural zeolite: equilibrium and kinetics. Environ Sci Pollut Res Int. 2022;29:79808-15. https://doi.org/10.1007/s11356-021-17452-z
8. Saxena R, Saxena M, Lochab A. Recent progress in nanomaterials for adsorptive removal of organic contaminants from wastewater. ChemistrySelect. 2020;5:335-53. https://doi.org/10.1002/slct.201903542
9. Gupta K, Joshi P, Gusain R, Khatri OP. Recent advances in adsorptive removal of heavy metal and metalloid ions by metal oxide-based nanomaterials. Coord Chem Rev. 2021;445:214100. https://doi.org/10.1016/j.ccr.2021.214100
10. Pereira Silva AL, Varela Júnior JD. Density functional theory study of Cu-modified B12N12 nanocage as a chemical sensor for carbon monoxide gas. Inorg Chem. 2022;62:1926-34. https://doi.org/10.1021/acs.inorgchem.2c01621
11. Hossain MR, Hasan MM, Shamim SU, Ferdous T, Hossain MA, Ahmed F. First-principles study of the adsorption of chlormethine anticancer drug on C24, B12N12 and B12C6N6 nanocages. Comput Theor Chem. 2021;1197:113156. https://doi.org/10.1016/j.comptc.2021.113156
12. Wu S, Li L, Liang Q, Gao H, Tang T, Tang Y. A DFT study of sulforaphane adsorption on the group III nitrides (B12N12, Al12N12 and Ga12N12) nanocages. J Biomol Struct Dyn. 2024;42:12730-41. https://doi.org/10.1080/07391102.2023.2272755
13. Jiao X, Lin J, Zhang R, Deng T, Yu C, Chen M, et al. Constructing of porous boron nitride granules for dynamic adsorption of CO_2. Sep Purif Technol. 2025;355:131727. https://doi.org/10.1016/j.seppur.2023.125219
14. Sikri N, Behera B, Kumar A, Kumar V, Pandey OP, Mehta J, et al. Recent advancements on 2D nanomaterials as emerging paradigm for the adsorptive removal of microcontaminants. Adv Colloid Interface Sci. 2025;331:103441. https://doi.org/10.1016/j.cis.2025.103441
15. de Sousa Sousa N, Silva AL, Silva AC, de Jesus Gomes Varela Júnior J. Cu-modified B12N12 nanocage as a chemical sensor for nitrogen monoxide gas: a density functional theory study. J Nanopart Res. 2023;25:248. https://doi.org/10.1007/s11051-023-05898-w
16. Benjamin I, Louis H, Okon GA, Qader SW, Afahanam LE, Fidelis CF, et al. Transition metal-decorated B12N12-X (X = Au, Cu, Ni, Os, Pt, and Zn) nanoclusters as biosensors for carboplatin. ACS Omega. 2023;8:10006-21. https://doi.org/10.1021/acsomega.2c07250
17. Gürer ES, Kaya S, Katin KP. Computational evaluation of Ni@B12N12 and Ti@B12N12 endohedral clusters as carriers for melphalan and sulforaphane anticancer drugs. J Mol Liq. 2025;427:127457. https://doi.org/10.1016/j.molliq.2025.127457
18. Janjua MR. Prediction and understanding: quantum chemical framework of transition metals enclosed in a B12N12 inorganic nanocluster for adsorption and removal of DDT from the environment. Inorg Chem. 2021;60:10837-47. https://doi.org/10.1021/acs.inorgchem.1c01760
19. Saadh MJ, Hsu C, Kareem RA, Jafarova AM, Zareii A, Edalat M, et al. Computational assessments of 5-Fluorocytosine (Flucytosine) antifungal adsorption onto a fullerene oxide nanocage for engineering a potential drug delivery platform. Chem Rev Lett. 2025;8:547-54.
20. Najafi F, Sattari Alamdar S, Vaziri E. Fullerene (C20) as a Sensor for the Detection of Nordazepam: DFT Simulations. J Med Med Chem. 2025;1(1):18-23. https://doi.org/10.22034/jmedchem.2025.526412.1004
21. Behjatmanesh-Ardakani R, Rzayev R. Hydrogen assisted SO_2 dissociation on the Pt-doped graphene quantum dot surface: a non-periodic DFT study. Chem

Rev Lett. 2025;8:178-86. https://doi.org/10.22034/crl.2024.489135.1476
22. Behjatmanesh-Ardakani R, Magkoev TT. SO_2 adsorption and its direct proportional dissociation on the Cu(100), Cu(110), and Cu(111) surfaces: a periodic DFT study. Chem Rev Lett. 2024;7:873-83. https://doi.org/10.22034/crl.2024.467740.1380
23. Mirderikvand N, Mahboubi-Rabbani M. A DFT Study on Citalopram Adsorption on the Surface of B12N12. J Chem Tech. 2025;1(3):90-5. https://doi.org/10.22034/jchemtech.2025.538393.1015
24. Mouna A, Hayat EO, Loubna H, Mouad BNM, Mohamed RC, Walid I, et al. Spectroscopic analysis and theoretical comparison of the reactivity of 6-amino-3(R)benzophenone reactions with acetylacetone. Chem Rev Lett. 2024;7:942-56. https://doi.org/10.22034/crl.2024.463313.1356
25. Mahdi MS, Mushtaq H, Hasan DF, Bahir H, Idan A, Hassan, et al. Electronic and optical properties of 2D VFeSb: case study by DFT. Chem Rev Lett. 2024;7:964-71. https://doi.org/10.22034/crl.2024.455831.1333
26. Abrahi Vahed S. B12N12 as a Sensor for the Detection of Nordazepam. Med Med Chem. 2024;1(1):14-9. https://doi.org/10.22034/medmedchem.2024.474845.1008
27. Behnia A, Jalali Sarvestani MR, Abdulmutaleb Ibrahim A, Mahdi MS. DFT studies on the nalidixic acid interactions with C8B6N6 nanocluster. Chem Rev Lett. 2024;7:993-1000. https://doi.org/10.22034/crl.2024.478064.1418
28. Behjatmanesh-Ardakani R, Rzayev R. Pd- and Pt-doped graphene quantum dots for SO_2 adsorption and dissociation: a non-periodic DFT study. Chem Rev Lett. 2024;7:1022-30. https://doi.org/10.22034/crl.2024.474971.1412
29. Jameel RK, Al-Anbari HA, Mansoor AS, Kadhem AH, Bahair H, Behmagham F, et al. Characterization of tetramethyl guanidinium 4-nitro phenoxide (TMG-NP) and tetraphenyl guanidinium 4-nitro phenoxide (TPG-NP) as new ionic liquids (ILs) using DFT and ab initio. Chem Rev Lett. 2024;7:661-76. https://doi.org/10.22034/crl.2024.465452.1368
30. Ekoro IA, Osharode ME. Computational Insights into Aporphine Alkaloids as Inhibitors of Lassa fever Virus: A Molecular Modelling and DFT Approach. Med Med Chem. 2025;Forthcoming. https://doi.org/10.22034/medmedchem.2025.544010.1049
31. Al-Sattar Dawood AA, Abdul Hussein AH, Al-Shami KR, Azizi B, Thabit R, MH, et al. Electronic and magnetic structure of monolayer MnAs (111): a case study by DFT. Chem Rev Lett. 2024;7:373-9. https://doi.org/10.22034/crl.2024.448436.1312
32. Dennington R, Keith TA, Millam JM. GaussView, Version 6.1. Shawnee Mission, KS: Semichem Inc.; 2016.
33. Frisch MJ, Trucks GW, Schlegel HB, Scuseria GE, Robb MA, Cheeseman JR, et al. Gaussian 16, Revision C.01. Wallingford CT: Gaussian, Inc.; 2016.
34. Orio M, Pantazis DA, Neese F. Density functional theory. Photosynth Res. 2009;102:443-53. https://doi.org/10.1007/s11120-009-9404-8
35. Rassolov VA, Pople JA, Ratner MA, Windus TL. 6-31G* basis set for atoms K through Zn. J Chem Phys. 1998;109:1223-9. https://doi.org/10.1063/1.476673
36. Tirado-Rives J, Jorgensen WL. Performance of B3LYP density functional methods for a large set of organic molecules. J Chem Theory Comput. 2008;4:297-306. https://doi.org/10.1021/ct700248k
37. Samavat S, Ghiasi R, Mohtat B. Conductor-like polarizable continuum model (CPCM) solvation analysis in a N-heterocyclic carbene complex of stannocene. Inorg Chem Res. 2021;5:257-64.
38. Hoseyni SJ, Karbakhshzadeh A, Moshtaghi Zonouz A, Husseen B. Computational investigation on interaction between graphene nanostructure BC3 and antiparkinson drug amantadine: possible sensing study of BC3 and its doped derivatives on amantadine. Chem Rev Lett. 2024;7:380-7. https://doi.org/10.22034/crl.2024.454413.1328
39. Abrahi Vahed S. Fullerene (C20) as a Sensor for Detection of Midazolam: Theoretical Insights. J Med Med Chem. 2025;1(3):106-10. doi:10.22034/jmedchem.2025.547513.1019.
40. Alimohammadi F, Rezanejade Bardajee G, Monfared A. The sensing behavior of MgO nanotube to thiopropamine drug via DFT investigation. Chem Rev Lett. 2024;7:513-21. https://doi.org/10.22034/crl.2024.457011.1335
41. Mohammadi B, Jalali Sarvestani MR. A comparative computational investigation on amantadine adsorption on the surfaces of pristine, C-, Si-, and Ga-doped aluminum nitride nanosheets. J Chem Lett. 2023;4:66-70. https://doi.org/10.22034/jchemlett.2023.388369.1107
42. Hsian RL, Hussin VK, Hamad OA, Kareem RO. Theoretical Study Chlorohydroquinone with substituted lithium via Quantum Computation Methods. Chem Res Tech. 2024;1(2):73-7. https://doi.org/10.2234/chemrestec.2024.448968.1009
43. John A, Uzairu A, Shallangwa G, Adamu UBA, S. Theoretical investigation and design of novel cephalosporin-based inhibitors of a DD-carboxypeptidase enzyme of Salmonella typhimurium. J Chem Lett. 2023;4:52-8. https://doi.org/10.22034/jchemlett.2022.361586.1085
44. Iorhuna F, Ayuba AM, Nyijime AT. Comparative study of skimmianine as an adsorptive inhibitor on Al (110) and Fe (111) crystal surface using DFT and simulation method. J Chem Lett. 2023;4:148-55. https://doi.org/10.22034/jchemlett.2023.398506.1117
45. Uzah T, Timothy M, Mbonu IJ. Insight into synergistic corrosion inhibition of thiourea and $ZnCl_2$ on mild steel: experimental and theoretical approaches. J Chem Lett. 2024;4:211-21. https://doi.org/10.22034/jchemlett.2024.413932.1135
46. Ahmadi R. Furazolidone Adsorption on the Surface of B12N12: DFT Simulations. J Med Med Chem. 2025;1(3):100-5. https://doi.org/10.22034/jmedchem.2025.547065.1018
47. Kareem RO, Hamad OA, Kebiroglu H, Mohammed BA. Spectroscopic properties and computational studies of phosphosilicate-doped compounds including (F, Cl, Br). J Chem Lett. 2024;5:159-67. https://doi.org/10.22034/jchemlett.2024.467720.1212
48. Issofa P, Eric N Njankwa, Gabriel C S K, Junior Ulrich B B J, Emadak A. Theoretical Mechanistic and Kinetic Study on the [1. 5]-H Shift in (Z)-hexa-1,3-diene. Chem Res Tech. 2024;1(2):89-94. https://doi.org/10.22034/chemrestec.2024.449583.1012
49. Rafiee MA, Javaheri M. Theoretical study of benzoquinone derivatives as organic cathode materials in lithium-ion batteries. J Chem Lett. 2025;6:166-74. https://doi.org/10.22034/jchemlett.2025.516569.1295